Review

Conformational Mobility of Voltage-Gated Ion Channels

Ekaterina Kravchuk , Elizaveta Trifonova , Olga S. Sokolova *

Posted Date: 9 September 2024

doi: 10.20944/preprints202409.0642.v1

Keywords: voltage-gated ion channels; conformation; membrane mimetics; cryoelectron microscopy; in situ analysis; coordinated motion

Review

Conformational Mobility of Voltage-Gated Ion Channels

Ekaterina Kravchuk [1], Elizaveta Trifonova [1] and Olga S. Sokolova [1,2] *

[1] Lomonosov Moscow University, 119234, Moscow, Russia; kravchuk.ev.15@gmail.com; trifonova.elizaveta@gmail.com
[2] Shenzhen MSU-BIT University, 518172, Shenzhen, Guangdong Province, P.R.C.; sokolova@mail.bio.msu.ru
* Correspondence: sokolova@mail.bio.msu.ru

Abstract: Structural biology has a strong interest in ion channels, a diverse group of membrane proteins. This group has long remained difficult to study, but much progress has been made in recent decades with improvements in biochemical methods and computational procedures. Voltage-gated ion channels undergo conformational changes upon functioning, and multiple models of activation mechanisms were proposed based on experimental data. This review focuses on the structural studies of the functioning of voltage-gated ion channels, which are accompanied by conformational changes in proteins, and the methodological advances that allow their observation. Modern experimental methods that allow obtaining ion channel proteins in specific functional states are discussed, including cryoelectron microscopy and cryoelectron tomography. Finally, new algorithms for studying the conformational mobility of proteins have been developed, which help to better understand the mechanisms of ion channel domain movements.

Keywords: voltage-gated ion channels; conformation; membrane mimetics; cryoelectron microscopy; *in situ* analysis; coordinated motion

1. Introduction

Ion channels are a functionally important and extensive class of transmembrane proteins that play an important role in cell life. In excitable tissues, they are involved in the maintenance of homeostasis and resting potential, as well as in the development of action potential [1,2]. A number of studies demonstrate the regulatory role of ion channels in processes such as cell differentiation [3–5], cell growth [6–8], apoptosis [7], neurotransmitter release [9], and hormone release [8]. Diseases caused by the disfunction of ion channels can have consequences such as ataxia, epilepsy, hereditary migraines, heart rhythm abnormalities, hormone secretion disorders, osteopetrosis, development of cancerous tumors, etc [6,10–17]. Thus, the study of ion channel functioning is of vital importance for medicine, including personalized medicine. Interest in this group of proteins has led to the development of a number of biochemical and biophysical approaches for the study of ion channels.

In recent years, methods for studying ion channels have been developing rapidly. Purification to preserve the membrane environment, protocols for creating polarized vesicles to observe individual channel states are being developed, and structural biology approaches that allow the observation of conformational changes are being refined. In this review we address a number of solved problems related to ion channel performance and method improvement.

2. Topology and Classification of Cation Channels

Ion channels have a modular structure, with most ion channels comprising of three key functional modules [18,19]:

(i) A pore domain (PD) with a narrow selective filter that conducts ions of a certain type;
(ii) A gate that regulates the opening and closing of a channel;

 doi:10.20944/preprints202409.0642.v1

(iii) Sensors that respond to external signals. In cationic voltage-gated channels, four repetitive subunits are radially arranged around the pore [20]. The transmembrane α-subunit of Na_v and Ca_v channels consists of four transmembrane domains comprising of S1-S6 helices, encoded by a single polypeptide chain (Fig. 1A). Helixes S1-S4 form the voltage-gated domain, while S4, the voltage sensor, being rich in positively charged amino acid residues, changes its position upon changing the membrane potential. The S5 and S6 helixes form a pore domain [2,21,22].

Potassium channels are tetramers, subdivided into four groups depending on the structural features of their monomers [23] (Fig. 1B):

(i) K_v (voltage-gated) possess six transmembrane helices (S1-S6), with S1-S4 forming a potential-sensing domain and S5-S6 – a pore domain;

(ii) K_{ir} (internally rectifying) through which ions pass easily into the cell, but not out; they have two transmembrane helices,

(iii) K_{2P} (bipore delayed rectification), with four transmembrane helices,

(iiii) K_{Ca} (calcium-activated), have six transmembrane helices, similar to those of K_v.

K_v transmembrane helices are conserved, whereas cytoplasmic regulatory domains are structurally distinct in different families, fulfilling different functions [24].

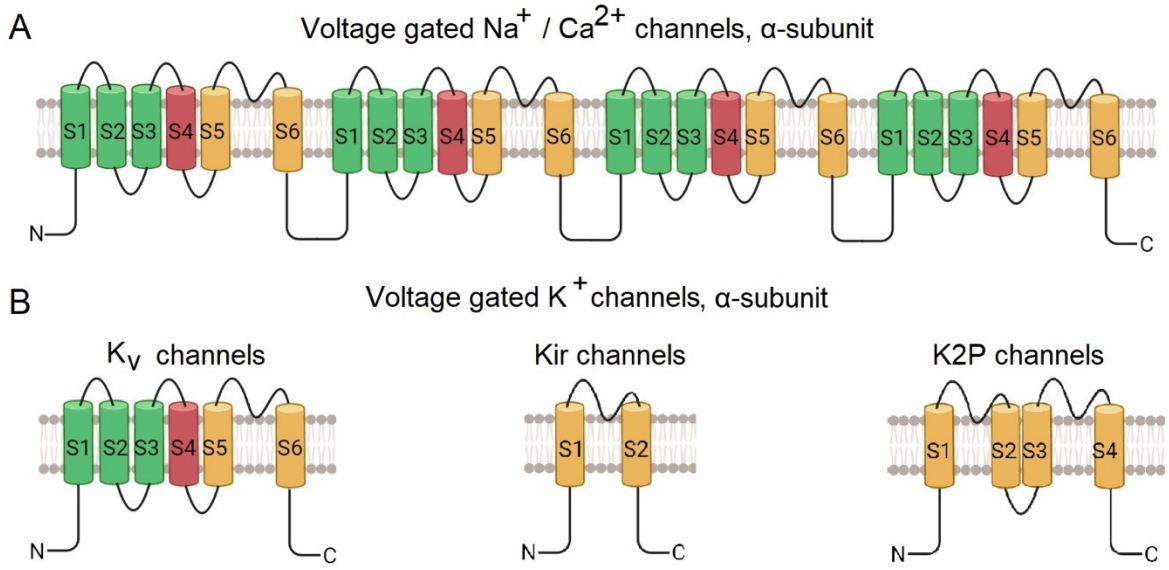

Figure 1. Diagram of the structure of the α-subunit of voltage-gated ion channels. A – sodium channels, B – calcium channels, C – potassium channels [25].

Voltage-gated ion channels function following the "all-or-nothing" law, i.e., they are either in a state of total ionic conductance, or zero conductance [26]. Three basic functional states are known: closed (with the potential sensor lowered and the pore closed), open (with the potential sensor raised), and inactivated (closed even when the potential sensor is raised) (Fig. 2) [27]. Several transition models describe open channel transitions to the inactivated (Fig. 2A) or to the closed state (Fig. 2B).

 doi:10.20944/preprints202409.0642.v1

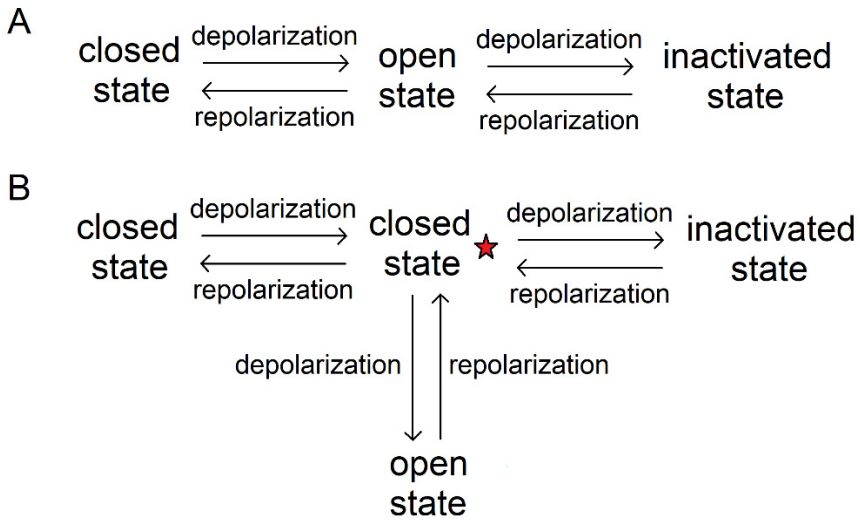

Figure 2. Transition from one key state of the ion channel to another. A – inactivation from an open state, B – inactivation from a closed state [28].

For a long time, experimental reconstructions of ion channels in intermediate conformational states have been lacking, however their presence was assumed. A highly conserved site (charge transfer center, CTC) of two negatively charged residues and phenylalanine was found in a voltage-gated domain, which presumably binds the positively charged amino acid of S4 and catalyzes the movement of the potential sensor [29]. For the K_v1.2 channel, five states: open, closed, and three intermediate ones, where different positively charged amino acids were bound to the CTC, have been suggested by a group of French researchers [30]. In addition, in 2011, a K_v channel deactivation model (MDM) was proposed to describe the intermediate conformations of the *Shaker* channel, among which an open, two intermediate, closed, and a deep closed state were identified [31]; also reviewed in [27].

To date, a number of intermediate states have been established for few channels. For example, PIP_2 binding is required for K_v7.1 activation [32,33]. For K_v7.1, a model with an intermediate S4 position was constructed based on experimental data [34]. For K_v10.2, reconstructions of several intermediate states were obtained, and, in addition, the closed state of K_v10.2 was able to be subdivided into several distinct sub-states [35].

Two topology variants have been described for voltage-gated ion channels [34,36]: (i) "domain-swapped" channels, in which the voltage-sensing domain (VSD) is spatially closer to the neighboring PD, and a long S4-S5 linker is present. These include K_v1-8, Na_v, Ca_v channels [37–39]. (ii) “non-domain-swapped" channels, where the VSD is spatially closer to the PD of the same polypeptide chain, with a relatively short S4-S5 linker. These include K_v7-12 channels. Attachment of low-molecular-weight ligands is required for the activation of these channels [34,40–42].

The development of methods that would allow the study of intermediate states of the ion channels, as well as continuous, rather than discrete, conformational changes based on experimental data, is of high relevancy.

3. Experimental Prerequisites for Studying the Structure of Ion Channels

Structural studies provide the most thorough information on the peculiarities of protein macromolecule functioning. Membranes of different cells are unique in composition; to study ion channels in a near native state, membrane-modulating media are used [28,43]. The selection of a suitable membrane mimetic is a separate non-trivial task that is solved for each specific protein. The main types of membrane mimetics used are detergents (micelles, bicelles), amphipoles, nanodiscs, and amphiphilic SMA polymers (lipodiscs) [43,44] (Fig. 3). Recently, studies of channels incorporated directly into liposomes [45,46] have become widespread. All these methods will be reviewed below.

 doi:10.20944/preprints202409.0642.v1

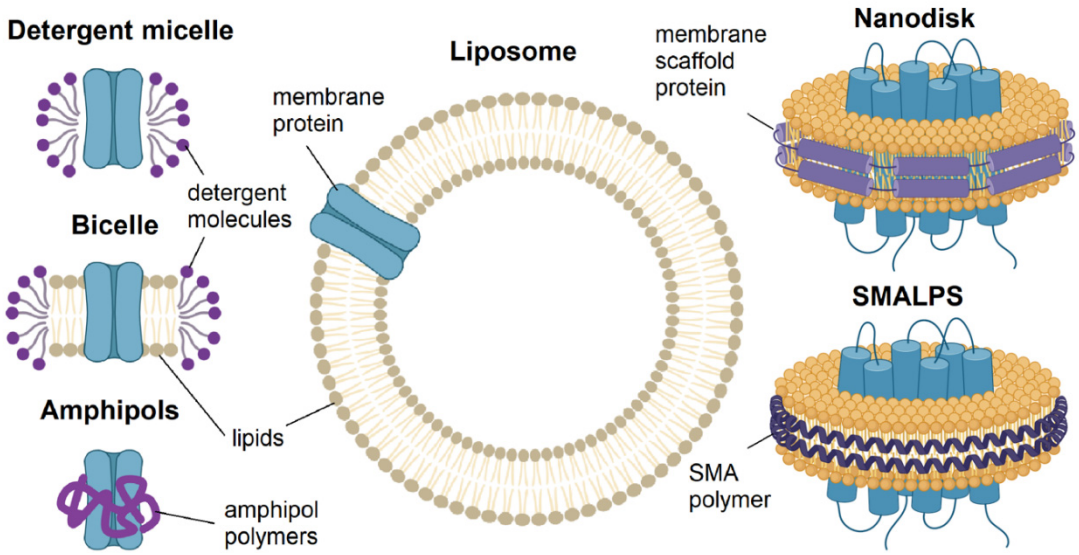

Figure 3. Schematic representation of different membrane mimetics used in structural studies of membrane proteins [44].

3.1. Purification Strategies

3.1.1. Detergents: Micelles and Bicelles

Detergents are amphiphilic substances including hydrophilic and hydrophobic parts that form micelles (Fig. 3). According to their nature of action, they are distinguished as hard detergents that destroy protein-protein interactions (e.g., SDS) and soft detergents (e.g., TX-100, DDM, Tween, and OG). Zwitter-ionic, ionic, and non-ionic detergents are differentiated by their chemical nature. When selecting a detergent, general detergent properties: charge, fatty acid chain length, hydrophilic-hydrophobic balance, and other parameters, should be taken into account, as well as the selection of the optimal concentration, depending on the critical micelle concentration (CMC) [47–49]. Using detergents, the first reconstructions of the structures with the near atomic resolution were obtained for Kv7.1 [32], Kv10.1 [50], Kv11.1 [51], and a number of other ion channels [52].

The membrane-modulating properties of detergent micelles, which may differ significantly in spatial organization from the cell membrane, can be improved by the addition of phospholipids. The resulting particles, comprising of detergent and phospholipids, have been named bicelles (Fig. 4) [53,54]. Bicelles have been used for various structural studies of ion channels [55–57], however they did not gain as much popularity as detergents, nanodiscs, and SMALPs, especially for cryoEM studies. The main problems in using bicelles are that the total lipid concentration can affect the size and geometry of a bicelle and that insufficient bilayer size may lead to the risk of membrane protein disruption [58].

Preprints.org (www.preprints.org) | NOT PEER-REVIEWED | Posted: 9 September 2024 doi:10.20944/preprints202409.0642.v1

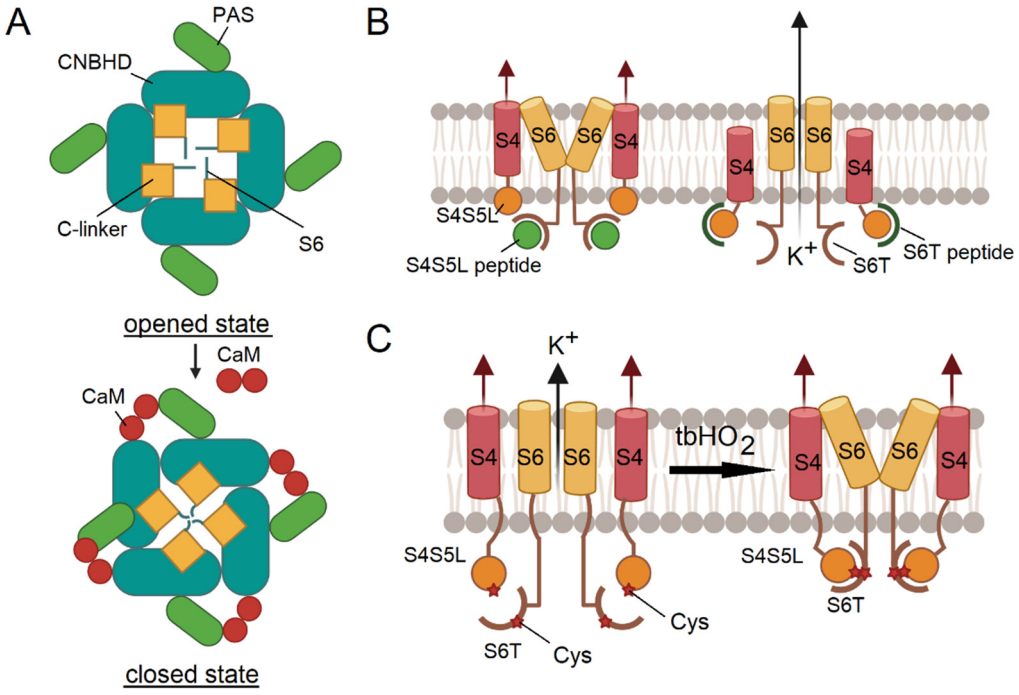

Figure 4. A – schematic representation of EAG1 closure upon interaction with calmodulin in the presence of calcium ions [50]. The channel is viewed from the cytoplasmic side. B – S4-S5 peptide mimics endogenous interaction of S4-S5 with S6, blocking the channel in a closed conformation (left). The S6T peptide (green) binds to endogenous S4-S5L and limits its blocking effect (right). C – introduction of cysteine substitutions (shown with asterisks) into S4-S5L and S6T, followed by treatment with the oxidative reagent $tbHO_2$, leads to the formation of disulfide bonds and the fixation of the channel in its closed conformation [37].

3.1.2. Polymers: Amphipols, Nanodiscs, Lipodiscs

Amphipols (Fig. 3) are artificially synthetized amphipathic polymers comprising of hydrophobic and hydrophilic parts, in which groups are randomly arranged, but their ratio is preserved. Amphipols embrace the hydrophobic regions of membrane proteins, making them hydrophilic [59]. Membrane proteins can be transferred to amphipols after solubilization in detergents, but this approach leads to heterogeneity of the samples [60].

Nanodiscs are proteolipid systems consisting of two copies of an amphipathic α-helical membrane scaffold protein (MSP) wrapped around a small disc of the lipid bilayer that they stabilize (Fig. 3). In recent years, nanodiscs have become most popular for studying membrane proteins, due to their monodispersity, adjustable lipid composition, and high stability. Membrane proteins can be assembled into nanodiscs by co-dissolving the protein, lipid, and MSP in a single detergent [61–65].

The application of styrene-maleic acid (SMA) copolymers has been a methodological breakthrough in the development of membrane mimetics for the study of membrane proteins. This amphiphilic copolymer solubilizes biological membranes to form SMALPs (Styrene-Maleic Acid-Lipid Particles), a.k.a. lipodiscs, disc-shaped structures surrounding the membrane protein of interest; thus, preserving its native lipid environment (Fig. 3)[66–70]. This recently introduced promising approach has already been actively applied into practice [68,70,71].

3.1.3. Lipids: Liposomes and Membrane Vesicles

Liposomes (Fig. 3) are multilamellar membrane vesicles consisting of several concentric lipid bilayers [72,73]. A number of methods for their preparation are known, including dispersion of lipid films in aqueous solution, ultrasound treatment, and the extrusion of lipid dispersion through polycarbonate membranes [74]. Liposomes are diverse in bilayer number, size, and composition. By

 doi:10.20944/preprints202409.0642.v1

varying the lipid composition of liposomes, it is possible to approximate their properties to those of the cell membrane and place the protein under study in a close to native environment, which is a key advantage of liposomes [75].

Recently, studies on the structure of ion channels in vesicles obtained directly from cell membranes after ultrasonic treatment have emerged. The advantage of this approach is that the membrane protein remains in its native environment. The vesicles are purified by ion exchange chromatography. Both the proteins from intracellular membranes and the proteins from the plasma membrane are purified [76]. Recently, the Slo1 potassium channel embedded in membrane vesicles was examined by cryo-electron tomography [77], and reconstructions of Slo1 embedded into the intracellular and plasma membranes were obtained at 3.8 Å and 2.7 Å resolution, respectively. This procedure resulted in about 90% of the vesicles being derived from intracellular membranes. The proteins in the vesicles can be orientated in two ways, for the extracellular and intracellular parts different tags can be used for purification.

A method for studying ion channels in polarized proteoliposomes is currently being actively developed, which is discussed in detail in section 3.4.

3.2. Methods for Obtaining Ion Channels in Specific Functional States

For a long time, the study of ion channels by structural biology methods was hampered by difficulties in 3D crystallization for X-ray analysis [78]. A number of models describing the transition from one state of ion channels to another have been proposed, based on indirect studies; current models are based on structural data [27]. Studies of mutations leading to channelopathies have provided important information on the role of specific sites of ion channels for their functioning [79]. Other approaches, such as the introduction of cysteine substitutions [80,81], fluorescent methods (FRET, LRET, VCF) [82,83], and molecular modelling [84,85], have also provided a better understanding of the mechanisms of conformational transitions.

Pioneering structural studies of ion channels were performed by R. MacKinnon's group in late 1990-s by X-ray diffraction analysis [86]. A number of ion channel structures have been obtained through crystallization in the lipid cubic phase [87,88]. Now it is obvious that cryo-electron microscopy is best suited to work with membrane proteins, due to their large size, difficulty in crystallization, and requirement for lipid environment preservation [89].

Membrane disruption during cell lysis results in depolarization, leading to the voltage sensor S4 of the ion channel to be in a raised position, thus, many structures of the voltage-gated potassium channels were solved in open or semi-open states [34,51,90,91]. Therefore, for many ion channels, only structures for a fraction of the conformational states have been obtained to date [92–95], while homology modelling has been applied to study the mechanism of switching between states.

For the $K_v10.2$ channel, structures in different states (including several closed states) were recently obtained through the use of advanced data analysis algorithms for particles of proteins solubilized with detergents, however, the authors suggest the presence of other states, such as a deep closed state at -70 mV [35].

Various approaches can be used to obtain channel structures that are unlikely to occur when the membrane is destroyed: approaches based on the understanding of the biology of individual proteins and methods suitable for one family of channels, but that may be inapplicable for another. Let us consider some of these methods using specific ion channels as examples.

3.2.1. Application of Ion Channel Modulators

Calmodulin (CaM) was shown to bind to $K_v10.1$ (EAG1) in the presence of Ca^{2+} to inhibit ionic conductance, through closing the channel pore (Fig. 4A) [96,97]. Each of the four EAG1 subunit has three CaM contacting sites that form two binding sites [97].

By binding simultaneously to cytoplasmic CMBD and PAS domains from neighboring subunits, CaM acts as a molecular clamp, pulling the two domains together and, thus, changing their orientation [50]. By using CaM-mediated channel inhibition, the group of R. MacKinnon obtained the structure of the $K_v10.1$ channel in a closed state with a resolution of 3.8 Å [50].

 doi:10.20944/preprints202409.0642.v1

3.2.2. Peptide Binding Mimics the Functional States of Ion Channels

For a number of voltage-gated channels, for which the ligand-receptor model of action has been proposed, a method of fixing the channel in a particular state through peptides that mimic the S4-S5 linker ("ligand") or the C-terminal portion of the S6 ("receptor") can be used. With peptides mimicking the S4-S5 linker, the channel is closed in the presence of depolarization and voltage sensor bias. Similarly, with a peptide mimicking the C-terminus of S6, the channel can be secured in the open position without membrane depolarization (Fig. 4B).

Experimentally, it was shown that it is possible to open K_v11.1 [37] and Na_v1.4 [98] and close K_v11.1 [37] and K_v10.1 [38] channels using chemical cross-linking to form disulfide bonds.

Interestingly, we have found a new mutation in the K_v7.1 channel [14] that disrupts the poly-Lys strip in the proximal part of the highly conserved cytoplasmic A–B linker of the channel, which was not shown before to be crucial for the correct functioning of K_v7 channels [99,100] and, thus, it was removed in several structural studies [101,102]. This mutation leads to the development of the LQT syndrome in the patient, demonstrating the importance of a flexible structural part.

3.2.3. Chemical Cross-Linking and Coordination of Metal Ions

Subsequently, a method to secure the channel in a closed state was proposed. When cysteines are introduced into the neighboring positions of the S4-S5 linker and the C-terminus of S6, disulfide bonds are formed under oxidative conditions to close the channel. Thus, for the D540C-L666C mutant variant of hERG, it was shown that, in the presence of an oxidizer, it does not conduct current when voltage is applied (Fig. 4C) [37]. The same is applicable for the Na_v [98], K_v7.1 [39] and K_v10.2 channels [38].

Chemical cross-linking of PD and VSD cysteines has also been used for domain-swapped channels. The closed Na_vAb channel reconstruction with a resolution of 4.0 Å was obtained [103].

The coordination of the IIB-group of metal ions by cysteines has been used to reconstruct the resting state structure of K_v4.2 [28]. In this study, four channel states corresponding to the states of the inactivation model through the closed state were characterized and a possible mechanism of inactivation (through the disruption of channel symmetry) was described. The mechanism includes C4 symmetry breakdown while the channel becomes C2-symmetric. The C2 symmetric pore enables the creation of narrow constrictions along the ion conduction pathway. It is interesting that the closed-state inactivation of the K_v4.2 channel operates through a mechanism that differs from other voltage-gated ion channels [28].

3.3. Application of Toxins with Voltage-Gated Ion Channels

Some toxins, such as scorpion α-toxin, affect the voltage-gated domain in such a way that the potential sensor is blocked in the lowered state. When this toxin was exposed to the Na_v1.7-Na_vPaS chimeric channel (with the human Na_v1.7 scorpion α-toxin binding site transferred to the cockroach Na_vPaS channel to simplify expression), a structure was obtained with the potential sensor downregulated at near-atomic resolution, whereas in the apo state it was upregulated. Comparison of these reconstructions revealed displacements of the potential sensor during activation [104]. A similar effect is exerted by protoxin-II of the Peruvian green velvet tarantula. It was used to reconstruct the human Na_v1.7 in complex with a toxin with a voltage sensor in the 'down' position [105].

3.4. New Approach – Polarized Membrane Vesicles

To screen potential drugs acting on potassium ion channels, a method was developed using proteoliposomes incorporating the channel of interest, an ionophore (e.g. CCCP (carbonyl cyanide m-chlorophenylhydrazone) conducting protons) (Fig. 5A). Vesicles prepared in a buffer rich in potassium ions are transferred to an isotonic buffer with sodium ions, resulting in a concentration gradient and an outflow of potassium ions from the vesicle through the potassium channel, which is balanced by an influx of protons through the ionophore. The fluorescent dye ACMA, whose

 doi:10.20944/preprints202409.0642.v1

fluorescence is quenched by protons, is used to visualize the process, with the proton passing through the lipid bilayer before binding and not after attachment (Fig. 5A).

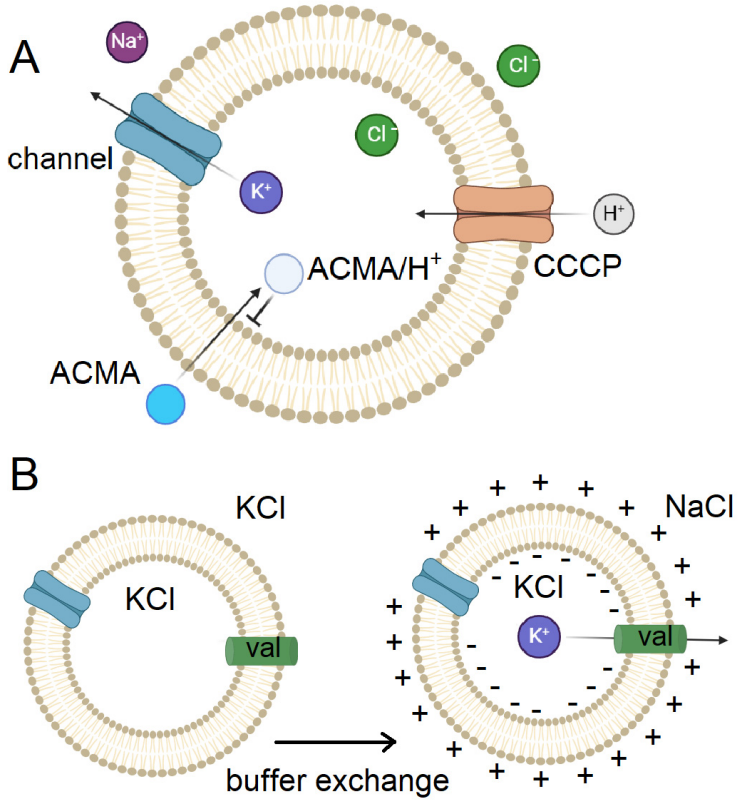

Figure 5. Use of liposomes for the study of ion channels. A – schematic of proteoliposome for drug screening [106], B – obtaining polarized membrane vesicles that include the Eag channel [107].

Thus, if the potassium channel is open, the medium inside the vesicle is acidified and the quenched dye accumulates inside the vesicle and the fluorescence signal drops, whereas if the channel is closed or blocked, no drop in fluorescence was observed. When a potassium ionophore is added to the system, even in the absence of potassium current through the channel, potassium can escape from the vesicle and the fluorescence drops in this case as well [106].

Subsequently, a similar system was used by R. MacKinnon's group to create polarized vesicles and to study ion channels within these vesicles during membrane polarization. In this approach, vesicles are formed in a buffer containing KCl and transferred to a buffer with isotonic NaCl solution on a column; polarization is achieved by the potassium current conducting ionophore valinomycin (Fig. 5B). CCCP is also present in the system, making it possible to visualize the process using ACMA. Using this system allowed us to study the Eag channel with the potential sensor omitted and the potential sensor in the intermediate state by cryo-electron microscopy [107]. The same method was used to study Kv7.1, which allowed us to build a model of the activation of this channel upon PIP_2 binding. Models were constructed with the potential sensor omitted and the potential sensor in the intermediate state, which allowed to determine that, upon opening, the ligand binding site appears first, then PIP_2 attaches, and the pore is opened [34].

The described mechanism of channel closure is potentially applicable for structural analysis of ion channels in intermediate states, for which reconstructions have not yet been obtained. The structural analysis of the bacterial channel NaChBac under an electrochemical gradient was performed by cryoET and subtomogram averaging. This study explores the limits of studying small ion channels in polarized proteoliposomes [46].

 doi:10.20944/preprints202409.0642.v1

4. Advanced Structural Methods for the Study of Voltage-Gated Ion Channel Conformational Changes

4.1. Cryo-Electron Microscopy

In the past decade, cryo-electron microscopy (cryoEM) has become one of the leading methods for studying the patterns of ion channel functioning [108,109]. With the revolution in cryoEM resolution, the number of structures obtained by this method has increased dramatically. Currently, more than 1000 ion channel structures are present in PDB: both cationic and anionic, from a variety of cellular compartments collected from a range of organisms using a variety of purification methods. Furthermore, the resolution obtained for ion channels using this method approaches atomic resolution [92,108,110]. Advances that have led to the resolution revolution in cryoEM include the advent of direct electron detection detectors and the development of data analysis algorithms [108,109]. Most of the published structures have a resolution in the range of 3 – 4 Å, the best resolution for ion channels is currently in the order of 1.8 Å. This result was obtained for the calcium-activated human chloride channel hBest2 [111].

The interaction of ion channels with their lipid environment is being actively investigated [112], aided by the development of biochemical methods for channel solubilization and purification (see Section 3.1). A number of studies demonstrate that lipids can be sequenced and can interact specifically with hydrophobic regions of ion channels [64,113,114]. For some cases, the regulatory role of lipids has been shown [115]. For example, phosphoinositide lipids serve as negative modulators of TRPV1, whose release from the binding pocket is a critical step towards activation [116]. PIP_2 binding is a prerequisite for the ability to activate $K_v7.1$ [34,41]. As another example, membrane lipids affect the conformation and function of the two-pore potassium channel TREK1 [117].

In addition to the structures of ion channels in different conformational states, cryo-electron microscopy was also used to study:

- chimeric channels [118–120],
- mutant channels [121–126],
- channels in complex with regulatory proteins, like calmodulin [41,125,127–130],
- channels in complex with low molecular weight ligands, both natural [131–134], and synthetic [33,135–137].

Obtaining ion channel structures in complex with ligands is not only of fundamental interest, but is also of practical significance for medicine [110].

Thus, at present, cryoEM is one of the most convenient, informative structural biology methods applicable to ion channel studies.

4.2. Development of New Algorithms for the Identifucation of Distinct Conformational States of Ion Channels

There are a number of tools in cryoEM available to identify distinct conformational states during the analysis of cryo-electron microscopy data, including specifying multiple class types during initial model building, 2D and 3D classification, and heterogeneous refinement [138–140], which pertain to discrete state methods. Simultaneously, in recent years, new algorithms for analyzing conformational homogeneity that investigate continuous conformational changes have been developed [141–143]. For this purpose, PCA-based methods using data subsets [144], PPCA-based methods [145,146], and covariance estimation-based methods [147,148] were proposed.

In 2021, the developers of the cryoSPARC software package implemented the 3D Variability Analysis (3DVA) algorithm [146]. 3DVA allows the visualization of movements of individual structural elements of protein macromolecules, which offers new biological information based on cryoEM data. 3DVA is designed as a variant of the expectation-maximization algorithm for the probabilistic principal component method (PPCA). 3DVA resolves continuous conformational changes, allows the identification of new biologically relevant patterns from cryoEM data, and simplifies the analysis of conformational heterogeneity [146].

 doi:10.20944/preprints202409.0642.v1

The 3DVA algorithm was used to analyze the conformational mobility of ion channels, including the complex of the potential-dependent sodium channel $Na_v1.7$ with the region of the immunoglobulin molecule that binds antigen (Na_v-Fab) [146]. A 3D analysis of variability was performed with a low-pass filter with a 3 Å resolution cut-off and six components of variability. Fig. 7A shows part of the variability components. The first component describes the bending of the two transmembrane subunits and the movement of bound Fab's. The outer transmembrane helices move left and right, while the Fab's alternately approach and move away from each other. The second component reflects the lateral bending of the four α-helices of the cytoplasmic domain. The sixth component shows the up-and-down movements of the two subunits not associated with Fabs. High resolution of peripheral transmembrane helices could not be obtained in this work [149], 3DVA provides an explanation of what causes such limitations.

3DVA was also used to study potassium channels, namely the lysosomal channel TMEM175, which is evolutionarily distant from all known channels. The algorithm allowed for the characterization of the conformational heterogeneity and the identification of two states, which were further used for iterative rounds of heterogeneous refinement. Reconstructions at 2.6 and 3.0 Å resolution were constructed, providing a better understanding of the mechanism of channel selectivity and opening [150] (Fig. 7B).

Methods that in the long term may allow a transition to energy computation are also being actively developed. Thus, the RECOVAR method [152], a PCA-based method computed using regularized covariance estimation, is similar in principle to 3DVA, but has a number of differences. For example, RECOVAR allows automatic regularization, which makes it more stable than 3DVA when choosing incorrect parameters, as well as faster and less computationally demanding [152].

Recently, the 3D Flexible Refinement (3D Flex) algorithm [153], a model of continuous heterogeneity based on a deep neural network, was implemented in cryoSPARC. 3DFlex directly exploits the knowledge that protein conformational variability is often the result of physical processes, given physical constraints. From 2D image data, the 3DFlex model learns a single canonical 3D map, latent coordinate vectors that define positions on the protein conformational landscape, and a flow generator that, given the latent position as input, outputs a 3D strain field. This deformation field transforms the canonical map into the corresponding conformations to explain the experimental images. When applied to experimental data, 3DFlex studies non-rigid motion spanning several orders of magnitude, while preserving high-resolution details of the secondary structure. In addition, 3DFlex resolves canonical maps, which are an improvement over conventional refinement methods. 3DFlex was used to analyze the TRPV1 ion channel (Fig. 6C) [151].

Two types of flexible, coordinated motion among the four peripheral domains of the ion channel have been recorded. Along the first latent dimension, each pair of opposing subunits bends towards one another, while the other pair bends sideways. The second involves all four subunits twisting concentrically around the axis of the channel pore. In both cases, the most peripheral helices move about 6 Å. Both movements are non-rigid and involve the bending of substantial regions of protein density. Improved alignment using this algorithm improved the resolution of the peripheral regions of the protein from 4 to 3.2 Å [151].

The cryoDRGN method [143], based on the use of deep neural networks, also provides interesting results. This method has been applied in a number of studies of ion channels, including the characterization of the mobility of the N-terminal domain of the ligand-dependent DeCLIC channel and the role of this domain in the regulation of channel function [154].

Preprints.org (www.preprints.org) | NOT PEER-REVIEWED | Posted: 9 September 2024 doi:10.20944/preprints202409.0642.v1

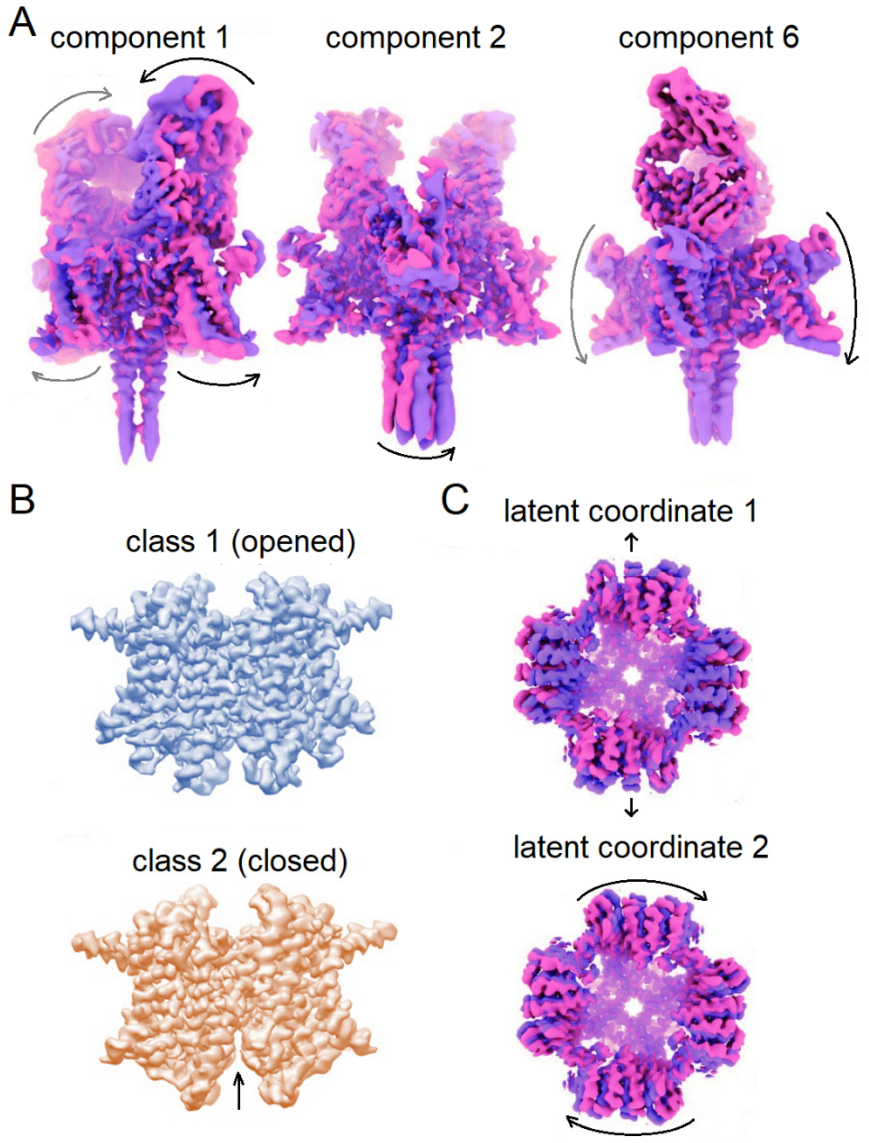

Figure 6. A – 3DVA results with six variability components (three shown) on images of 300,759 $Na_v1.7$ channel particles [146], B – classes extracted for TMEM175 using 3D classification and 3DVA [150], C – 3DFlex results for TRPV1 [151].

4.3. Cryo-Electron Tomography

In cryo-electron tomography (cryoET), the sample is physically rotated around an axis perpendicular to the optical path of the microscope at different angles. The data obtained are used to construct a reconstruction – a 3D tomogram. Subtomogram averaging, a computational procedure that uses subvolumes extracted from the tomogram and that includes individual particles, is used to obtain a reconstruction of macromolecules [155,156]. Solutions for working with the membrane and membrane-associated proteins are also being developed, both experimental (e.g., using extracellular vesicles as a platform for structure determination [157]) and computational [158–160], as well as new algorithms and pipelines for data analysis [65,155,156,161–164].

In 2015, a reconstruction of the 5-HT3 receptor, a ligand-driven ion channel, was obtained using cryoET, with a resolution of 12 Å [165]. In 2020, a paper was published on the structure of the ryanodine receptor (RyR1) in native membranes, a resolution of the order of 12.6 Å was obtained. In this work, it was shown that, upon activation by ryanodine and calcium, a change in the receptor conformation led to a change in the membrane curvature, which may play an important role for

 doi:10.20944/preprints202409.0642.v1

channel opening [166]. More recently, for RyR1, the resolution was improved to 9.1 Å using a combination of subtomogram averaging and single particle analysis [167]. Regarding potential-dependent ion channels, a reconstruction of the bacterial NaChBac sodium channel in polarized proteoliposomes was obtained in 2023 with a resolution of ~16 Å [46].

Thus, the study of ion channels by cryoET provides an opportunity to analyze their function in native membranes, and, although the resolution has not yet reached the same orders of magnitude as in single particle cryoEM, new data analysis pipelines and algorithms that have emerged in recent years have a great potential.

5. Conclusions

Within the last decade, new approaches and algorithms have rapidly been developed to study the structure and conformational changes of voltage-gated ion channels. CryoEM is well suited for determining the 3D structures, but until recently its data analysis techniques were inefficient for reconstructing flexible domains and conformational changes in protein. After 2D or 3D averaging, the resolution of the mobile domain is usually lower than for stable regions of a protein [168]. Recently, a number of tools became available to identify distinct conformational states during the analysis of cryo-EM data, including 3D classification and heterogeneous refinement [138–140], as well as 3D Flexible Refinement [146]. *In situ* methods became more widespread, which will help identify unique structures of ion channels in the membrane.

Author Contributions: Conceptualization, O.S.S. and E.K.; writing—original draft preparation, E.K.; writing—review and editing, O.S.S., E.T.; supervision, O.S.S.; funding acquisition, O.S.S. All authors have read and agreed to the published version of the manuscript.

Funding: This research was funded by RSF, grant 22-14-00088.

Institutional Review Board Statement: Not applicable.

Informed Consent Statement: Not applicable.

Acknowledgments: OSS is the head of an innovative drug development team based on structural biology and bioinformatics at Shenzhen MSU-BIT University, Guangdong province, P.R.C. (2022KCXTD034).

Conflicts of Interest: The authors declare no conflicts of interest.

References

1. Kim, D.M.; Nimigean, C.M. Voltage-Gated Potassium Channels: A Structural Examination of Selectivity and Gating. *Cold Spring Harb Perspect Biol* **2016**, *8*, a029231, doi:10.1101/cshperspect.a029231.
2. Catterall, W.A.; Lenaeus, M.J.; Gamal El-Din, T.M. Structure and Pharmacology of Voltage-Gated Sodium and Calcium Channels. *Annu. Rev. Pharmacol. Toxicol.* **2020**, *60*, 133–154, doi:10.1146/annurev-pharmtox-010818-021757.
3. Chen, L.; Hassani Nia, F.; Stauber, T. Ion Channels and Transporters in Muscle Cell Differentiation. *IJMS* **2021**, *22*, 13615, doi:10.3390/ijms222413615.
4. Prevarskaya, N.; Skryma, R.; Bidaux, G.; Flourakis, M.; Shuba, Y. Ion Channels in Death and Differentiation of Prostate Cancer Cells. *Cell Death Differ* **2007**, *14*, 1295–1304, doi:10.1038/sj.cdd.4402162.
5. Mauro, TheodoraM.; Isseroff, R.R.; Lasarow, R.; Pappone, PamelaA. Ion Channels Are Linked to Differentiation in Keratinocytes. *J. Membarin Biol.* **1993**, *132*, doi:10.1007/BF00235738.
6. Becchetti, A. Ion Channels and Transporters in Cancer. 1. Ion Channels and Cell Proliferation in Cancer. *American Journal of Physiology-Cell Physiology* **2011**, *301*, C255–C265, doi:10.1152/ajpcell.00047.2011.
7. Lang, F.; Föller, M.; Lang, K.S.; Lang, P.A.; Ritter, M.; Gulbins, E.; Vereninov, A.; Huber, S.M. Ion Channels in Cell Proliferation and Apoptotic Cell Death. *J Membrane Biol* **2005**, *205*, 147–157, doi:10.1007/s00232-005-0780-5.
8. Chen, C.; Vincent, J.-D.; Clarke, I.J. Ion Channels and the Signal Transduction Pathways in the Regulation of Growth Hormone Secretion. *Trends in Endocrinology & Metabolism* **1994**, *5*, 227–233, doi:10.1016/1043-2760(94)P3080-Q.
9. Carbone, E.; Calorio, C.; Vandael, D.H.F. T-Type Channel-Mediated Neurotransmitter Release. *Pflugers Arch - Eur J Physiol* **2014**, *466*, 677–687, doi:10.1007/s00424-014-1489-z.

10. Bianchi, L.; Wible, B.; Arcangeli, A.; Taglialatela, M.; Morra, F.; Castaldo, P.; Crociani, O.; Rosati, B.; Faravelli, L.; Olivotto, M.; et al. Herg Encodes a K+ Current Highly Conserved in Tumors of Different Histogenesis: A Selective Advantage for Cancer Cells? *Cancer Res* **1998**, *58*, 815–822.
11. Imbrici, P.; Liantonio, A.; Camerino, G.M.; De Bellis, M.; Camerino, C.; Mele, A.; Giustino, A.; Pierno, S.; De Luca, A.; Tricarico, D.; et al. Therapeutic Approaches to Genetic Ion Channelopathies and Perspectives in Drug Discovery. *Front. Pharmacol.* **2016**, *7*, doi:10.3389/fphar.2016.00121.
12. Li, B.; Karlova, M.; Zhang, H.; Pustovit, O.B.; Mai, L.; Novoseletsky, V.; Podolyak, D.; Zaklyazminskaya, E.V.; Abramochkin, D.V.; Sokolova, O.S. A Mutation in the Cardiac KV7.1 Channel Possibly Disrupts Interaction with Yotiao Protein. *Biochemical and Biophysical Research Communications* **2024**, *714*, 149947, doi:10.1016/j.bbrc.2024.149947.
13. Abramochkin, D.; Li, B.; Zhang, H.; Kravchuk, E.; Nesterova, T.; Glukhov, G.; Shestak, A.; Zaklyazminskaya, E.; Sokolova, O.S. Novel Gain-of-Function Mutation in the Kv11.1 Channel Found in the Patient with Brugada Syndrome and Mild QTc Shortening. *Biochemistry Moscow* **2024**, *89*, 543–552, doi:10.1134/S000629792403012X.
14. Karlova, M.; Abramochkin, D.V.; Pustovit, K.B.; Nesterova, T.; Novoseletsky, V.; Loussouarn, G.; Zaklyazminskaya, E.; Sokolova, O.S. Disruption of a Conservative Motif in the C-Terminal Loop of the KCNQ1 Channel Causes LQT Syndrome. *IJMS* **2022**, *23*, 7953, doi:10.3390/ijms23147953.
15. Zaklyazminskaya, E.; Polyak, M.; Shestak, A.; Sadekova, M.; Komoliatova, V.; Kiseleva, I.; Makarov, L.; Podolyak, D.; Glukhov, G.; Zhang, H.; et al. Variable Clinical Appearance of the Kir2.1 Rare Variants in Russian Patients with Long QT Syndrome. *Genes* **2022**, *13*, 559, doi:10.3390/genes13040559.
16. Karlova, M.; Rusinova, V.; Abramochkin, D.; Zaklyazminskaya, E.; Sokolova, O. Novel Kv7.1 Missense Mutation Lys422Glu Leads to the Development of LQT Syndrome. *Microsc Microanal* **2021**, *27*, 1742–1743, doi:10.1017/S1431927621006371.
17. Zhang, H.; Glukhov, G.S.; Pustovit, K.B.; Kacher, Yu.G.; Rusinova, V.S.; Kiseleva, I.I.; Komolyatova, V.N.; Makarov, L.M.; Zaklyazminskaya, E.V.; Sokolova, O.S. Phenotypic Manifestations of Val93Ile Missense Mutation and Its Influence on Kir2.1 Channel Functioning. *Moscow Univ. Biol.Sci. Bull.* **2021**, *76*, 142–146, doi:10.3103/S0096392521030056.
18. Minor, Jr, D.L. Searching for Interesting Channels: Pairing Selection and Molecular Evolution Methods to Study Ion Channel Structure and Function. *Mol. BioSyst.* **2009**, *5*, 802, doi:10.1039/b901708a.
19. Yu, F.H.; Yarov-Yarovoy, V.; Gutman, G.A.; Catterall, W.A. Overview of Molecular Relationships in the Voltage-Gated Ion Channel Superfamily. *Pharmacol Rev* **2005**, *57*, 387–395, doi:10.1124/pr.57.4.13.
20. Gouaux, E.; MacKinnon, R. Principles of Selective Ion Transport in Channels and Pumps. *Science* **2005**, *310*, 1461–1465, doi:10.1126/science.1113666.
21. Findeisen, F.; Minor, Jr., D.L. Progress in the Structural Understanding of Voltage-Gated Calcium Channel (Ca v) Function and Modulation. *Channels* **2010**, *4*, 459–474, doi:10.4161/chan.4.6.12867.
22. De Lera Ruiz, M.; Kraus, R.L. Voltage-Gated Sodium Channels: Structure, Function, Pharmacology, and Clinical Indications. *J. Med. Chem.* **2015**, *58*, 7093–7118, doi:10.1021/jm501981g.
23. MacKinnon, R. Potassium Channels. *FEBS Letters* **2003**, *555*, 62–65, doi:10.1016/S0014-5793(03)01104-9.
24. Islas, L.D. Functional Diversity of Potassium Channel Voltage-Sensing Domains. *Channels* **2016**, *10*, 202–213, doi:10.1080/19336950.2016.1141842.
25. Huang, Q.; Zhu, W.; Gao, X.; Liu, X.; Zhang, Z.; Xing, B. Nanoparticles-Mediated Ion Channels Manipulation: From Their Membrane Interactions to Bioapplications. *Advanced Drug Delivery Reviews* **2023**, *195*, 114763, doi:10.1016/j.addr.2023.114763.
26. Evolution of Ionic Channels of Biological Membranes. *Molecular Biology and Evolution* **1989**, doi:10.1093/oxfordjournals.molbev.a040562.
27. Grizel, A.V.; Glukhov, G.S.; Sokolova, O.S. Mechanisms of Activation of Voltage-Gated Potassium Channels. *Acta Naturae* **2014**, *6*, 10–26, doi:10.32607/20758251-2014-6-4-10-26.
28. Ye, W.; Zhao, H.; Dai, Y.; Wang, Y.; Lo, Y.; Jan, L.Y.; Lee, C.-H. Activation and Closed-State Inactivation Mechanisms of the Human Voltage-Gated KV4 Channel Complexes. *Molecular Cell* **2022**, *82*, 2427-2442.e4, doi:10.1016/j.molcel.2022.04.032.
29. Tao, X.; Lee, A.; Limapichat, W.; Dougherty, D.A.; MacKinnon, R. A Gating Charge Transfer Center in Voltage Sensors. *Science* **2010**, *328*, 67–73, doi:10.1126/science.1185954.
30. Delemotte, L.; Tarek, M.; Klein, M.L.; Amaral, C.; Treptow, W. Intermediate States of the Kv1.2 Voltage Sensor from Atomistic Molecular Dynamics Simulations. *Proc. Natl. Acad. Sci. U.S.A.* **2011**, *108*, 6109–6114, doi:10.1073/pnas.1102724108.
31. Vargas, E.; Bezanilla, F.; Roux, B. In Search of a Consensus Model of the Resting State of a Voltage-Sensing Domain. *Neuron* **2011**, *72*, 713–720, doi:10.1016/j.neuron.2011.09.024.
32. Sun, J.; MacKinnon, R. Cryo-EM Structure of a KCNQ1/CaM Complex Reveals Insights into Congenital Long QT Syndrome. *Cell* **2017**, *169*, 1042-1050.e9, doi:10.1016/j.cell.2017.05.019.

33. Ma, D.; Zhong, L.; Yan, Z.; Yao, J.; Zhang, Y.; Ye, F.; Huang, Y.; Lai, D.; Yang, W.; Hou, P.; et al. Structural Mechanisms for the Activation of Human Cardiac KCNQ1 Channel by Electro-Mechanical Coupling Enhancers. *Proc. Natl. Acad. Sci. U.S.A.* **2022**, *119*, e2207067119, doi:10.1073/pnas.2207067119.
34. Mandala, V.S.; MacKinnon, R. The Membrane Electric Field Regulates the PIP 2 -Binding Site to Gate the KCNQ1 Channel. *Proc. Natl. Acad. Sci. U.S.A.* **2023**, *120*, e2301985120, doi:10.1073/pnas.2301985120.
35. Zhang, M.; Shan, Y.; Pei, D. Mechanism Underlying Delayed Rectifying in Human Voltage-Mediated Activation Eag2 Channel. *Nat Commun* **2023**, *14*, 1470, doi:10.1038/s41467-023-37204-6.
36. Barros, F.; De La Peña, P.; Domínguez, P.; Sierra, L.M.; Pardo, L.A. The EAG Voltage-Dependent K+ Channel Subfamily: Similarities and Differences in Structural Organization and Gating. *Front. Pharmacol.* **2020**, *11*, 411, doi:10.3389/fphar.2020.00411.
37. Malak, O.A.; Es-Salah-Lamoureux, Z.; Loussouarn, G. hERG S4-S5 Linker Acts as a Voltage-Dependent Ligand That Binds to the Activation Gate and Locks It in a Closed State. *Sci Rep* **2017**, *7*, 113, doi:10.1038/s41598-017-00155-2.
38. Malak, O.A.; Gluhov, G.S.; Grizel, A.V.; Kudryashova, K.S.; Sokolova, O.S.; Loussouarn, G. Voltage-Dependent Activation in EAG Channels Follows a Ligand-Receptor Rather than a Mechanical-Lever Mechanism. *Journal of Biological Chemistry* **2019**, *294*, 6506–6521, doi:10.1074/jbc.RA119.007626.
39. Choveau, F.S.; Abderemane-Ali, F.; Coyan, F.C.; Es-Salah-Lamoureux, Z.; Baró, I.; Loussouarn, G. Opposite Effects of the S4–S5 Linker and PIP2 on Voltage-Gated Channel Function: KCNQ1/KCNE1 and Other Channels. *Front. Pharmacol.* **2012**, *3*, doi:10.3389/fphar.2012.00125.
40. Zaydman, M.A.; Cui, J. PIP2 Regulation of KCNQ Channels: Biophysical and Molecular Mechanisms for Lipid Modulation of Voltage-Dependent Gating. *Front. Physiol.* **2014**, *5*, doi:10.3389/fphys.2014.00195.
41. Sun, J.; MacKinnon, R. Structural Basis of Human KCNQ1 Modulation and Gating. *Cell* **2020**, *180*, 340-347.e9, doi:10.1016/j.cell.2019.12.003.
42. Zhang, Q.; Zhou, P.; Chen, Z.; Li, M.; Jiang, H.; Gao, Z.; Yang, H. Dynamic PIP 2 Interactions with Voltage Sensor Elements Contribute to KCNQ2 Channel Gating. *Proc. Natl. Acad. Sci. U.S.A.* **2013**, *110*, 20093–20098, doi:10.1073/pnas.1312483110.
43. Popot, J.-L. Folding Membrane Proteins in Vitro: A Table and Some Comments. *Archives of Biochemistry and Biophysics* **2014**, *564*, 314–326, doi:10.1016/j.abb.2014.06.029.
44. Yeh, V.; Goode, A.; Bonev, B.B. Membrane Protein Structure Determination and Characterisation by Solution and Solid-State NMR. *Biology* **2020**, *9*, 396, doi:10.3390/biology9110396.
45. Antonenko, Y.N.; S. Gluhov, G.; M. Firsov, A.; D. Pogozheva, I.; Kovalchuk, S.I.; V. Pechnikova, E.; Kotova, E.A.; S. Sokolova, O. Gramicidin A Disassembles Large Conductive Clusters of Its Lysine-Substituted Derivatives in Lipid Membranes. *Phys. Chem. Chem. Phys.* **2015**, *17*, 17461–17470, doi:10.1039/C5CP02047F.
46. Chang, S.-Y.S.; Dijkman, P.M.; Wiessing, S.A.; Kudryashev, M. Determining the Structure of the Bacterial Voltage-Gated Sodium Channel NaChBac Embedded in Liposomes by Cryo Electron Tomography and Subtomogram Averaging. *Sci Rep* **2023**, *13*, 11523, doi:10.1038/s41598-023-38027-7.
47. Le Maire, M.; Champeil, P.; Møller, J.V. Interaction of Membrane Proteins and Lipids with Solubilizing Detergents. *Biochimica et Biophysica Acta (BBA) - Biomembranes* **2000**, *1508*, 86–111, doi:10.1016/S0304-4157(00)00010-1.
48. Garavito, R.M.; Ferguson-Miller, S. Detergents as Tools in Membrane Biochemistry. *Journal of Biological Chemistry* **2001**, *276*, 32403–32406, doi:10.1074/jbc.R100031200.
49. Sokolova, O. Structure of Cation Channels, Revealed by Single Particle Electron Microscopy. *FEBS Letters* **2004**, *564*, 251–256, doi:10.1016/S0014-5793(04)00254-6.
50. Whicher, J.R.; MacKinnon, R. Structure of the Voltage-Gated K + Channel Eag1 Reveals an Alternative Voltage Sensing Mechanism. *Science* **2016**, *353*, 664–669, doi:10.1126/science.aaf8070.
51. Wang, W.; MacKinnon, R. Cryo-EM Structure of the Open Human Ether-à-Go-Go -Related K + Channel hERG. *Cell* **2017**, *169*, 422-430.e10, doi:10.1016/j.cell.2017.03.048.
52. Lee, H.J.; Lee, H.S.; Youn, T.; Byrne, B.; Chae, P.S. Impact of Novel Detergents on Membrane Protein Studies. *Chem* **2022**, *8*, 980–1013, doi:10.1016/j.chempr.2022.02.007.
53. Prosser, R.S.; Evanics, F.; Kitevski, J.L.; Al-Abdul-Wahid, M.S. Current Applications of Bicelles in NMR Studies of Membrane-Associated Amphiphiles and Proteins ‧. *Biochemistry* **2006**, *45*, 8453–8465, doi:10.1021/bi060615u.
54. Sanders, C.R.; Landis, G.C. Reconstitution of Membrane Proteins into Lipid-Rich Bilayered Mixed Micelles for NMR Studies. *Biochemistry* **1995**, *34*, 4030–4040, doi:10.1021/bi00012a022.
55. Kim, D.M.; Dikiy, I.; Upadhyay, V.; Posson, D.J.; Eliezer, D.; Nimigean, C.M. Conformational Heterogeneity in Closed and Open States of the KcsA Potassium Channel in Lipid Bicelles. *Journal of General Physiology* **2016**, *148*, 119–132, doi:10.1085/jgp.201611602.
56. Biverståhl, H.; Lind, J.; Bodor, A.; Mäler, L. Biophysical Studies of the Membrane Location of the Voltage-Gated Sensors in the HsapBK and KvAP K+ Channels. *Biochimica et Biophysica Acta (BBA) - Biomembranes* **2009**, *1788*, 1976–1986, doi:10.1016/j.bbamem.2009.07.001.

57. Payandeh, J.; Scheuer, T.; Zheng, N.; Catterall, W.A. The Crystal Structure of a Voltage-Gated Sodium Channel. *Nature* **2011**, *475*, 353–358, doi:10.1038/nature10238.
58. Majeed, S.; Ahmad, A.B.; Sehar, U.; Georgieva, E.R. Lipid Membrane Mimetics in Functional and Structural Studies of Integral Membrane Proteins. *Membranes* **2021**, *11*, 685, doi:10.3390/membranes11090685.
59. Tribet, C.; Audebert, R.; Popot, J.-L. Amphipols: Polymers That Keep Membrane Proteins Soluble in Aqueous Solutions. *Proc. Natl. Acad. Sci. U.S.A.* **1996**, *93*, 15047–15050, doi:10.1073/pnas.93.26.15047.
60. Etzkorn, M.; Raschle, T.; Hagn, F.; Gelev, V.; Rice, A.J.; Walz, T.; Wagner, G. Cell-Free Expressed Bacteriorhodopsin in Different Soluble Membrane Mimetics: Biophysical Properties and NMR Accessibility. *Structure* **2013**, *21*, 394–401, doi:10.1016/j.str.2013.01.005.
61. Matthies, D.; Bae, C.; Toombes, G.E.; Fox, T.; Bartesaghi, A.; Subramaniam, S.; Swartz, K.J. Single-Particle Cryo-EM Structure of a Voltage-Activated Potassium Channel in Lipid Nanodiscs. *eLife* **2018**, *7*, e37558, doi:10.7554/eLife.37558.
62. Autzen, H.E.; Myasnikov, A.G.; Campbell, M.G.; Asarnow, D.; Julius, D.; Cheng, Y. Structure of the Human TRPM4 Ion Channel in a Lipid Nanodisc. *Science* **2018**, *359*, 228–232, doi:10.1126/science.aar4510.
63. Winterstein, L.-M.; Kukovetz, K.; Rauh, O.; Turman, D.L.; Braun, C.; Moroni, A.; Schroeder, I.; Thiel, G. Reconstitution and Functional Characterization of Ion Channels from Nanodiscs in Lipid Bilayers. *Journal of General Physiology* **2018**, *150*, 637–646, doi:10.1085/jgp.201711904.
64. Gao, Y.; Cao, E.; Julius, D.; Cheng, Y. TRPV1 Structures in Nanodiscs Reveal Mechanisms of Ligand and Lipid Action. *Nature* **2016**, *534*, 347–351, doi:10.1038/nature17964.
65. Shenkarev, Z.O.; Karlova, M.G.; Kulbatskii, D.S.; Kirpichnikov, M.P.; Lyukmanova, E.N.; Sokolova, O.S. Recombinant Production, Reconstruction in Lipid–Protein Nanodiscs, and Electron Microscopy of Full-Length α-Subunit of Human Potassium Channel Kv7.1. *Biochemistry Moscow* **2018**, *83*, 562–573, doi:10.1134/S0006297918050097.
66. Knowles, T.J.; Finka, R.; Smith, C.; Lin, Y.-P.; Dafforn, T.; Overduin, M. Membrane Proteins Solubilized Intact in Lipid Containing Nanoparticles Bounded by Styrene Maleic Acid Copolymer. *J. Am. Chem. Soc.* **2009**, *131*, 7484–7485, doi:10.1021/ja810046q.
67. Orwick-Rydmark, M.; Lovett, J.E.; Graziadei, A.; Lindholm, L.; Hicks, M.R.; Watts, A. Detergent-Free Incorporation of a Seven-Transmembrane Receptor Protein into Nanosized Bilayer Lipodisq Particles for Functional and Biophysical Studies. *Nano Lett.* **2012**, *12*, 4687–4692, doi:10.1021/nl3020395.
68. Glukhov, G.; Karlova, M.; Kravchuk, E.; Glukhova, A.; Trifonova, E.; Sokolova, O.S. Purification of Potassium Ion Channels Using Styrene–Maleic Acid Copolymers. In *Potassium Channels*; Furini, S., Ed.; Methods in Molecular Biology; Springer US: New York, NY, 2024; Vol. 2796, pp. 73–86 ISBN 978-1-07-163817-0.
69. Orekhov, P.S.; Bozdaganyan, M.E.; Voskoboynikova, N.; Mulkidjanian, A.Y.; Karlova, M.G.; Yudenko, A.; Remeeva, A.; Ryzhykau, Y.L.; Gushchin, I.; Gordeliy, V.I.; et al. Mechanisms of Formation, Structure, and Dynamics of Lipoprotein Discs Stabilized by Amphiphilic Copolymers: A Comprehensive Review. *Nanomaterials* **2022**, *12*, 361, doi:10.3390/nano12030361.
70. Karlova, M.G.; Voskoboynikova, N.; Gluhov, G.S.; Abramochkin, D.; Malak, O.A.; Mulkidzhanyan, A.; Loussouarn, G.; Steinhoff, H.-J.; Shaitan, K.V.; Sokolova, O.S. Detergent-Free Solubilization of Human Kv Channels Expressed in Mammalian Cells. *Chemistry and Physics of Lipids* **2019**, *219*, 50–57, doi:10.1016/j.chemphyslip.2019.01.013.
71. Sun, C.; Gennis, R.B. Single-Particle Cryo-EM Studies of Transmembrane Proteins in SMA Copolymer Nanodiscs. *Chemistry and Physics of Lipids* **2019**, *221*, 114–119, doi:10.1016/j.chemphyslip.2019.03.007.
72. Bangham, A.D. Lipid Bilayers and Biomembranes. *Annu. Rev. Biochem.* **1972**, *41*, 753–776, doi:10.1146/annurev.bi.41.070172.003541.
73. Bangham, A.D. Liposomes: The Babraham Connection. *Chemistry and Physics of Lipids* **1993**, *64*, 275–285, doi:10.1016/0009-3084(93)90071-A.
74. Woodle, M.C.; Papahadjopoulos, D. [9] Liposome Preparation and Size Characterization. In *Methods in Enzymology*; Elsevier, 1989; Vol. 171, pp. 193–217 ISBN 978-0-12-182072-5.
75. Wang, L.; Tonggu, L. Membrane Protein Reconstitution for Functional and Structural Studies. *Sci. China Life Sci.* **2015**, *58*, 66–74, doi:10.1007/s11427-014-4769-0.
76. Chorev, D.S.; Baker, L.A.; Wu, D.; Beilsten-Edmands, V.; Rouse, S.L.; Zeev-Ben-Mordehai, T.; Jiko, C.; Samsudin, F.; Gerle, C.; Khalid, S.; et al. Protein Assemblies Ejected Directly from Native Membranes Yield Complexes for Mass Spectrometry. *Science* **2018**, *362*, 829–834, doi:10.1126/science.aau0976.
77. Tao, X.; Zhao, C.; MacKinnon, R. Membrane Protein Isolation and Structure Determination in Cell-Derived Membrane Vesicles. *Proc. Natl. Acad. Sci. U.S.A.* **2023**, *120*, e2302325120, doi:10.1073/pnas.2302325120.
78. Hille, B.; Armstrong, C.M.; MacKinnon, R. Ion Channels: From Idea to Reality. *Nat Med* **1999**, *5*, 1105–1109, doi:10.1038/13415.
79. Catterall, W.A. Structure and Function of Voltage-Gated Ion Channels. *Trends in Neurosciences* **1993**, *16*, 500–506, doi:10.1016/0166-2236(93)90193-P.

80. Karlin, A.; Akabas, M.H. [8] Substituted-Cysteine Accessibility Method. In *Methods in Enzymology*; Elsevier, 1998; Vol. 293, pp. 123–145 ISBN 978-0-12-182194-4.
81. Liapakis, G.; Simpson, M.M.; Javitch, J.A. The Substituted-Cysteine Accessibility Method (SCAM) to Elucidate Membrane Protein Structure. *CP Neuroscience* **1999**, *8*, doi:10.1002/0471142301.ns0415s08.
82. Glauner, K.S.; Mannuzzu, L.M.; Gandhi, C.S.; Isacoff, E.Y. Spectroscopic Mapping of Voltage Sensor Movement in the Shaker Potassium Channel. *Nature* **1999**, *402*, 813–817, doi:10.1038/45561.
83. Martinac, B. Single-Molecule FRET Studies of Ion Channels. *Progress in Biophysics and Molecular Biology* **2017**, *130*, 192–197, doi:10.1016/j.pbiomolbio.2017.06.014.
84. Capener, C.E. Ion Channels: Structural Bioinformatics and Modelling. *Human Molecular Genetics* **2002**, *11*, 2425–2433, doi:10.1093/hmg/11.20.2425.
85. Tai, K.; Fowler, P.; Mokrab, Y.; Stansfeld, P.; Sansom, M.S.P. Chapter 12 Molecular Modeling and Simulation Studies of Ion Channel Structures, Dynamics and Mechanisms. In *Methods in Cell Biology*; Elsevier, 2008; Vol. 90, pp. 233–265 ISBN 978-1-59749-270-6.
86. Doyle, D.A.; Cabral, J.M.; Pfuetzner, R.A.; Kuo, A.; Gulbis, J.M.; Cohen, S.L.; Chait, B.T.; MacKinnon, R. The Structure of the Potassium Channel: Molecular Basis of K^+ Conduction and Selectivity. *Science* **1998**, *280*, 69–77, doi:10.1126/science.280.5360.69.
87. Cherezov, V.; Clogston, J.; Misquitta, Y.; Abdel-Gawad, W.; Caffrey, M. Membrane Protein Crystallization In Meso: Lipid Type-Tailoring of the Cubic Phase. *Biophysical Journal* **2002**, *83*, 3393–3407, doi:10.1016/S0006-3495(02)75339-3.
88. Cherezov, V.; Clogston, J.; Papiz, M.Z.; Caffrey, M. Room to Move: Crystallizing Membrane Proteins in Swollen Lipidic Mesophases. *Journal of Molecular Biology* **2006**, *357*, 1605–1618, doi:10.1016/j.jmb.2006.01.049.
89. Bai, X.; McMullan, G.; Scheres, S.H.W. How Cryo-EM Is Revolutionizing Structural Biology. *Trends in Biochemical Sciences* **2015**, *40*, 49–57, doi:10.1016/j.tibs.2014.10.005.
90. Selvakumar, P.; Fernández-Mariño, A.I.; Khanra, N.; He, C.; Paquette, A.J.; Wang, B.; Huang, R.; Smider, V.V.; Rice, W.J.; Swartz, K.J.; et al. Structures of the T Cell Potassium Channel Kv1.3 with Immunoglobulin Modulators. *Nat Commun* **2022**, *13*, 3854, doi:10.1038/s41467-022-31285-5.
91. Fan, X.; Huang, J.; Jin, X.; Yan, N. Cryo-EM Structure of Human Voltage-Gated Sodium Channel $Na_v1.6$. *Proc. Natl. Acad. Sci. U.S.A.* **2023**, *120*, e2220578120, doi:10.1073/pnas.2220578120.
92. Berman, H.M. The Protein Data Bank. *Nucleic Acids Research* **2000**, *28*, 235–242, doi:10.1093/nar/28.1.235.
93. Špačková, A.; Vávra, O.; Raček, T.; Bazgier, V.; Sehnal, D.; Damborský, J.; Svobodová, R.; Bednář, D.; Berka, K. ChannelsDB 2.0: A Comprehensive Database of Protein Tunnels and Pores in AlphaFold Era. *Nucleic Acids Research* **2024**, *52*, D413–D418, doi:10.1093/nar/gkad1012.
94. Ranjan, R.; Khazen, G.; Gambazzi, L.; Ramaswamy, S.; Hill, S.L.; Schürmann, F.; Markram, H. Channelpedia: An Integrative and Interactive Database for Ion Channels. *Front. Neuroinform.* **2011**, *5*, doi:10.3389/fninf.2011.00036.
95. Huang, J.; Pan, X.; Yan, N. Structural Biology and Molecular Pharmacology of Voltage-Gated Ion Channels. *Nat Rev Mol Cell Biol* **2024**, doi:10.1038/s41580-024-00763-7.
96. Schonherr, R. Inhibition of Human Ether a Go-Go Potassium Channels by Ca2+/Calmodulin. *The EMBO Journal* **2000**, *19*, 3263–3271, doi:10.1093/emboj/19.13.3263.
97. Ziechner, U.; Schönherr, R.; Born, A.; Gavrilova-Ruch, O.; Glaser, R.W.; Malesevic, M.; Küllertz, G.; Heinemann, S.H. Inhibition of Human *Ether à Go-go* Potassium Channels by Ca^{2+} /Calmodulin Binding to the Cytosolic N- and C-termini. *The FEBS Journal* **2006**, *273*, 1074–1086, doi:10.1111/j.1742-4658.2006.05134.x.
98. Malak, O.A.; Abderemane-Ali, F.; Wei, Y.; Coyan, F.C.; Pontus, G.; Shaya, D.; Marionneau, C.; Loussouarn, G. Up-Regulation of Voltage-Gated Sodium Channels by Peptides Mimicking S4-S5 Linkers Reveals a Variation of the Ligand-Receptor Mechanism. *Sci Rep* **2020**, *10*, 5852, doi:10.1038/s41598-020-62615-6.
99. Haitin, Y.; Wiener, R.; Shaham, D.; Peretz, A.; Cohen, E.B.-T.; Shamgar, L.; Pongs, O.; Hirsch, J.A.; Attali, B. Intracellular Domains Interactions and Gated Motions of IKS Potassium Channel Subunits. *EMBO J* **2009**, *28*, 1994–2005, doi:10.1038/emboj.2009.157.
100. Aivar, P.; Fernández-Orth, J.; Gomis-Perez, C.; Alberdi, A.; Alaimo, A.; Rodríguez, M.S.; Giraldez, T.; Miranda, P.; Areso, P.; Villarroel, A. Surface Expression and Subunit Specific Control of Steady Protein Levels by the Kv7.2 Helix A-B Linker. *PLoS ONE* **2012**, *7*, e47263, doi:10.1371/journal.pone.0047263.
101. Chang, A.; Abderemane-Ali, F.; Hura, G.L.; Rossen, N.D.; Gate, R.E.; Minor, D.L. A Calmodulin C-Lobe Ca2+-Dependent Switch Governs Kv7 Channel Function. *Neuron* **2018**, *97*, 836-852.e6, doi:10.1016/j.neuron.2018.01.035.
102. Sachyani, D.; Dvir, M.; Strulovich, R.; Tria, G.; Tobelaim, W.; Peretz, A.; Pongs, O.; Svergun, D.; Attali, B.; Hirsch, J.A. Structural Basis of a Kv7.1 Potassium Channel Gating Module: Studies of the Intracellular C-Terminal Domain in Complex with Calmodulin. *Structure* **2014**, *22*, 1582–1594, doi:10.1016/j.str.2014.07.016.
103. Wisedchaisri, G.; Tonggu, L.; McCord, E.; Gamal El-Din, T.M.; Wang, L.; Zheng, N.; Catterall, W.A. Resting-State Structure and Gating Mechanism of a Voltage-Gated Sodium Channel. *Cell* **2019**, *178*, 993-1003.e12, doi:10.1016/j.cell.2019.06.031.

104. Clairfeuille, T.; Cloake, A.; Infield, D.T.; Llongueras, J.P.; Arthur, C.P.; Li, Z.R.; Jian, Y.; Martin-Eauclaire, M.-F.; Bougis, P.E.; Ciferri, C.; et al. Structural Basis of α-Scorpion Toxin Action on Na v Channels. *Science* **2019**, *363*, eaav8573, doi:10.1126/science.aav8573.
105. Xu, H.; Li, T.; Rohou, A.; Arthur, C.P.; Tzakoniati, F.; Wong, E.; Estevez, A.; Kugel, C.; Franke, Y.; Chen, J.; et al. Structural Basis of Nav1.7 Inhibition by a Gating-Modifier Spider Toxin. *Cell* **2019**, *176*, 702-715.e14, doi:10.1016/j.cell.2018.12.018.
106. Su, Z.; Brown, E.C.; Wang, W.; MacKinnon, R. Novel Cell-Free High-Throughput Screening Method for Pharmacological Tools Targeting K + Channels. *Proc. Natl. Acad. Sci. U.S.A.* **2016**, *113*, 5748–5753, doi:10.1073/pnas.1602815113.
107. Mandala, V.S.; MacKinnon, R. Voltage-Sensor Movements in the Eag Kv Channel under an Applied Electric Field. *Proc. Natl. Acad. Sci. U.S.A.* **2022**, *119*, e2214151119, doi:10.1073/pnas.2214151119.
108. Kühlbrandt, W. The Resolution Revolution. *Science* **2014**, *343*, 1443–1444, doi:10.1126/science.1251652.
109. Egelman, E.H. The Current Revolution in Cryo-EM. *Biophysical Journal* **2016**, *110*, 1008–1012, doi:10.1016/j.bpj.2016.02.001.
110. Pliushcheuskaya, P.; Künze, G. Recent Advances in Computer-Aided Structure-Based Drug Design on Ion Channels. *IJMS* **2023**, *24*, 9226, doi:10.3390/ijms24119226.
111. Owji, A.P.; Wang, J.; Kittredge, A.; Clark, Z.; Zhang, Y.; Hendrickson, W.A.; Yang, T. Structures and Gating Mechanisms of Human Bestrophin Anion Channels. *Nat Commun* **2022**, *13*, 3836, doi:10.1038/s41467-022-31437-7.
112. Biou, V. Lipid-Membrane Protein Interaction Visualised by Cryo-EM: A Review. *Biochimica et Biophysica Acta (BBA) - Biomembranes* **2023**, *1865*, 184068, doi:10.1016/j.bbamem.2022.184068.
113. Long, S.B.; Tao, X.; Campbell, E.B.; MacKinnon, R. Atomic Structure of a Voltage-Dependent K+ Channel in a Lipid Membrane-like Environment. *Nature* **2007**, *450*, 376–382, doi:10.1038/nature06265.
114. Bergh, C.; Rovšnik, U.; Howard, R.; Lindahl, E. Discovery of Lipid Binding Sites in a Ligand-Gated Ion Channel by Integrating Simulations and Cryo-EM. *eLife* **2024**, *12*, RP86016, doi:10.7554/eLife.86016.3.
115. Ahmed, T.; Nisler, C.R.; Fluck, E.C.; Walujkar, S.; Sotomayor, M.; Moiseenkova-Bell, V.Y. Structure of the Ancient TRPY1 Channel from Saccharomyces Cerevisiae Reveals Mechanisms of Modulation by Lipids and Calcium. *Structure* **2022**, *30*, 139-155.e5, doi:10.1016/j.str.2021.08.003.
116. Arnold, W.R.; Mancino, A.; Moss, F.R.; Frost, A.; Julius, D.; Cheng, Y. Structural Basis of TRPV1 Modulation by Endogenous Bioactive Lipids. *Nat Struct Mol Biol* **2024**, doi:10.1038/s41594-024-01299-2.
117. Schmidpeter, P.A.M.; Petroff, J.T.; Khajoueinejad, L.; Wague, A.; Frankfater, C.; Cheng, W.W.L.; Nimigean, C.M.; Riegelhaupt, P.M. Membrane Phospholipids Control Gating of the Mechanosensitive Potassium Leak Channel TREK1. *Nat Commun* **2023**, *14*, 1077, doi:10.1038/s41467-023-36765-w.
118. Gao, S.; Valinsky, W.C.; On, N.C.; Houlihan, P.R.; Qu, Q.; Liu, L.; Pan, X.; Clapham, D.E.; Yan, N. Employing NaChBac for Cryo-EM Analysis of Toxin Action on Voltage-Gated Na + Channels in Nanodisc. *Proc. Natl. Acad. Sci. U.S.A.* **2020**, *117*, 14187–14193, doi:10.1073/pnas.1922903117.
119. Wisedchaisri, G.; Tonggu, L.; Gamal El-Din, T.M.; McCord, E.; Zheng, N.; Catterall, W.A. Structural Basis for High-Affinity Trapping of the NaV1.7 Channel in Its Resting State by Tarantula Toxin. *Molecular Cell* **2021**, *81*, 38-48.e4, doi:10.1016/j.molcel.2020.10.039.
120. Kschonsak, M.; Jao, C.C.; Arthur, C.P.; Rohou, A.L.; Bergeron, P.; Ortwine, D.F.; McKerrall, S.J.; Hackos, D.H.; Deng, L.; Chen, J.; et al. Cryo-EM Reveals an Unprecedented Binding Site for NaV1.7 Inhibitors Enabling Rational Design of Potent Hybrid Inhibitors. *eLife* **2023**, *12*, e84151, doi:10.7554/eLife.84151.
121. Lee, C.-H.; MacKinnon, R. Voltage Sensor Movements during Hyperpolarization in the HCN Channel. *Cell* **2019**, *179*, 1582-1589.e7, doi:10.1016/j.cell.2019.11.006.
122. Lu, Y.; Yu, M.; Jia, Y.; Yang, F.; Zhang, Y.; Xu, X.; Li, X.; Yang, F.; Lei, J.; Wang, Y.; et al. Structural Basis for the Activity Regulation of a Potassium Channel AKT1 from Arabidopsis. *Nat Commun* **2022**, *13*, 5682, doi:10.1038/s41467-022-33420-8.
123. Liu, S.; Zhao, Y.; Dong, H.; Xiao, L.; Zhang, Y.; Yang, Y.; Ong, S.T.; Chandy, K.G.; Zhang, L.; Tian, C. Structures of Wild-Type and H451N Mutant Human Lymphocyte Potassium Channel KV1.3. *Cell Discov* **2021**, *7*, 39, doi:10.1038/s41421-021-00269-y.
124. Li, S.; Wang, Y.; Wang, C.; Zhang, Y.; Sun, D.; Zhou, P.; Tian, C.; Liu, S. Cryo-EM Structure Reveals a Symmetry Reduction of the Plant Outward-Rectifier Potassium Channel SKOR. *Cell Discov* **2023**, *9*, 67, doi:10.1038/s41421-023-00572-w.
125. Whicher, J.R.; MacKinnon, R. Regulation of Eag1 Gating by Its Intracellular Domains. *eLife* **2019**, *8*, e49188, doi:10.7554/eLife.49188.
126. Lee, S.-N.; Cho, H.-J.; Jeong, H.; Ryu, B.; Lee, H.-J.; Kim, M.; Yoo, J.; Woo, J.-S.; Lee, H.H. Cryo-EM Structures of Human Cx36/GJD2 Neuronal Gap Junction Channel. *Nat Commun* **2023**, *14*, 1347, doi:10.1038/s41467-023-37040-8.
127. Vinayagam, D.; Quentin, D.; Yu-Strzelczyk, J.; Sitsel, O.; Merino, F.; Stabrin, M.; Hofnagel, O.; Yu, M.; Ledeboer, M.W.; Nagel, G.; et al. Structural Basis of TRPC4 Regulation by Calmodulin and Pharmacological Agents. *eLife* **2020**, *9*, e60603, doi:10.7554/eLife.60603.

128. Fluck, E.C.; Yazici, A.T.; Rohacs, T.; Moiseenkova-Bell, V.Y. Structural Basis of TRPV5 Regulation by Physiological and Pathophysiological Modulators. *Cell Reports* **2022**, *39*, 110737, doi:10.1016/j.celrep.2022.110737.
129. Singh, P.; Kumari, S.; Guldhe, A.; Misra, R.; Rawat, I.; Bux, F. Trends and Novel Strategies for Enhancing Lipid Accumulation and Quality in Microalgae. *Renewable and Sustainable Energy Reviews* **2016**, *55*, 1–16, doi:10.1016/j.rser.2015.11.001.
130. Barret, D.C.A.; Schuster, D.; Rodrigues, M.J.; Leitner, A.; Picotti, P.; Schertler, G.F.X.; Kaupp, U.B.; Korkhov, V.M.; Marino, J. Structural Basis of Calmodulin Modulation of the Rod Cyclic Nucleotide-Gated Channel. *Proc. Natl. Acad. Sci. U.S.A.* **2023**, *120*, e2300309120, doi:10.1073/pnas.2300309120.
131. Ma, D.; Zheng, Y.; Li, X.; Zhou, X.; Yang, Z.; Zhang, Y.; Wang, L.; Zhang, W.; Fang, J.; Zhao, G.; et al. Ligand Activation Mechanisms of Human KCNQ2 Channel. *Nat Commun* **2023**, *14*, 6632, doi:10.1038/s41467-023-42416-x.
132. Mathiharan, Y.K.; Glaaser, I.W.; Zhao, Y.; Robertson, M.J.; Skiniotis, G.; Slesinger, P.A. Structural Insights into GIRK2 Channel Modulation by Cholesterol and PIP2. *Cell Reports* **2021**, *36*, 109619, doi:10.1016/j.celrep.2021.109619.
133. Feng, S.; Dang, S.; Han, T.W.; Ye, W.; Jin, P.; Cheng, T.; Li, J.; Jan, Y.N.; Jan, L.Y.; Cheng, Y. Cryo-EM Studies of TMEM16F Calcium-Activated Ion Channel Suggest Features Important for Lipid Scrambling. *Cell Reports* **2019**, *28*, 567-579.e4, doi:10.1016/j.celrep.2019.06.023.
134. Huang, Y.; Roth, B.; Lü, W.; Du, J. Ligand Recognition and Gating Mechanism through Three Ligand-Binding Sites of Human TRPM2 Channel. *eLife* **2019**, *8*, e50175, doi:10.7554/eLife.50175.
135. Willegems, K.; Eldstrom, J.; Kyriakis, E.; Ataei, F.; Sahakyan, H.; Dou, Y.; Russo, S.; Van Petegem, F.; Fedida, D. Structural and Electrophysiological Basis for the Modulation of KCNQ1 Channel Currents by ML277. *Nat Commun* **2022**, *13*, 3760, doi:10.1038/s41467-022-31526-7.
136. Li, X.; Zhang, Q.; Guo, P.; Fu, J.; Mei, L.; Lv, D.; Wang, J.; Lai, D.; Ye, S.; Yang, H.; et al. Molecular Basis for Ligand Activation of the Human KCNQ2 Channel. *Cell Res* **2021**, *31*, 52–61, doi:10.1038/s41422-020-00410-8.
137. Zheng, Y.; Liu, H.; Chen, Y.; Dong, S.; Wang, F.; Wang, S.; Li, G.-L.; Shu, Y.; Xu, F. Structural Insights into the Lipid and Ligand Regulation of a Human Neuronal KCNQ Channel. *Neuron* **2022**, *110*, 237-247.e4, doi:10.1016/j.neuron.2021.10.029.
138. Verbeke, E.J.; Zhou, Y.; Horton, A.P.; Mallam, A.L.; Taylor, D.W.; Marcotte, E.M. Separating Distinct Structures of Multiple Macromolecular Assemblies from Cryo-EM Projections. *Journal of Structural Biology* **2020**, *209*, 107416, doi:10.1016/j.jsb.2019.107416.
139. Hu, M.; Yu, H.; Gu, K.; Wang, Z.; Ruan, H.; Wang, K.; Ren, S.; Li, B.; Gan, L.; Xu, S.; et al. A Particle-Filter Framework for Robust Cryo-EM 3D Reconstruction. *Nat Methods* **2018**, *15*, 1083–1089, doi:10.1038/s41592-018-0223-8.
140. Punjani, A.; Rubinstein, J.L.; Fleet, D.J.; Brubaker, M.A. cryoSPARC: Algorithms for Rapid Unsupervised Cryo-EM Structure Determination. *Nat Methods* **2017**, *14*, 290–296, doi:10.1038/nmeth.4169.
141. Sorzano, C.O.S.; Jiménez, A.; Mota, J.; Vilas, J.L.; Maluenda, D.; Martínez, M.; Ramírez-Aportela, E.; Majtner, T.; Segura, J.; Sánchez-García, R.; et al. Survey of the Analysis of Continuous Conformational Variability of Biological Macromolecules by Electron Microscopy. *Acta Crystallogr F Struct Biol Commun* **2019**, *75*, 19–32, doi:10.1107/S2053230X18015108.
142. Toader, B.; Sigworth, F.J.; Lederman, R.R. Methods for Cryo-EM Single Particle Reconstruction of Macromolecules Having Continuous Heterogeneity. *Journal of Molecular Biology* **2023**, *435*, 168020, doi:10.1016/j.jmb.2023.168020.
143. Donnat, C.; Levy, A.; Poitevin, F.; Zhong, E.D.; Miolane, N. Deep Generative Modeling for Volume Reconstruction in Cryo-Electron Microscopy. *Journal of Structural Biology* **2022**, *214*, 107920, doi:10.1016/j.jsb.2022.107920.
144. Penczek, P.A.; Kimmel, M.; Spahn, C.M.T. Identifying Conformational States of Macromolecules by Eigen-Analysis of Resampled Cryo-EM Images. *Structure* **2011**, *19*, 1582–1590, doi:10.1016/j.str.2011.10.003.
145. Tagare, H.D.; Kucukelbir, A.; Sigworth, F.J.; Wang, H.; Rao, M. Directly Reconstructing Principal Components of Heterogeneous Particles from Cryo-EM Images. *Journal of Structural Biology* **2015**, *191*, 245–262, doi:10.1016/j.jsb.2015.05.007.
146. Punjani, A.; Fleet, D.J. 3D Variability Analysis: Resolving Continuous Flexibility and Discrete Heterogeneity from Single Particle Cryo-EM. *Journal of Structural Biology* **2021**, *213*, 107702, doi:10.1016/j.jsb.2021.107702.
147. Katsevich, E.; Katsevich, A.; Singer, A. Covariance Matrix Estimation for the Cryo-EM Heterogeneity Problem. *SIAM J. Imaging Sci.* **2015**, *8*, 126–185, doi:10.1137/130935434.
148. Andén, J.; Singer, A. Structural Variability from Noisy Tomographic Projections. *SIAM J. Imaging Sci.* **2018**, *11*, 1441–1492, doi:10.1137/17M1153509.
149. Punjani, A.; Zhang, H.; Fleet, D.J. Non-Uniform Refinement: Adaptive Regularization Improves Single-Particle Cryo-EM Reconstruction. *Nat Methods* **2020**, *17*, 1214–1221, doi:10.1038/s41592-020-00990-8.

150. Oh, S.; Paknejad, N.; Hite, R.K. Gating and Selectivity Mechanisms for the Lysosomal K+ Channel TMEM175. *eLife* **2020**, *9*, e53430, doi:10.7554/eLife.53430.
151. Punjani, A.; Fleet, D.J. 3DFlex: Determining Structure and Motion of Flexible Proteins from Cryo-EM. *Nat Methods* **2023**, *20*, 860–870, doi:10.1038/s41592-023-01853-8.
152. Gilles, M.A.; Singer, A. Cryo-EM Heterogeneity Analysis Using Regularized Covariance Estimation and Kernel Regression 2023.
153. Punjani, A.; Fleet, D. 3D Flexible Refinement: Structure and Motion of Flexible Proteins from Cryo-EM. *Microscopy and Microanalysis* **2022**, *28*, 1218–1218, doi:10.1017/S1431927622005074.
154. Andén, O.; Rovsnik, U.; Lycksell, M.; Howard, R.J.; Lindahl, E.R. Structural Characterization of Regulation by a Dynamic N-Terminal Module in the Pentameric Ligand-Gated Ion Channel DeCLIC. *Biophysical Journal* **2024**, *123*, 394a, doi:10.1016/j.bpj.2023.11.2405.
155. Wan, W.; Briggs, J.A.G. Cryo-Electron Tomography and Subtomogram Averaging. In *Methods in Enzymology*; Elsevier, 2016; Vol. 579, pp. 329–367 ISBN 978-0-12-805382-9.
156. Pyle, E.; Zanetti, G. Current Data Processing Strategies for Cryo-Electron Tomography and Subtomogram Averaging. *Biochemical Journal* **2021**, *478*, 1827–1845, doi:10.1042/BCJ20200715.
157. Zeev-Ben-Mordehai, T.; Vasishtan, D.; Siebert, C.A.; Whittle, C.; Grünewald, K. Extracellular Vesicles: A Platform for the Structure Determination of Membrane Proteins by Cryo-EM. *Structure* **2014**, *22*, 1687–1692, doi:10.1016/j.str.2014.09.005.
158. Lamm, L.; Righetto, R.D.; Wietrzynski, W.; Pöge, M.; Martinez-Sanchez, A.; Peng, T.; Engel, B.D. MemBrain: A Deep Learning-Aided Pipeline for Detection of Membrane Proteins in Cryo-Electron Tomograms. *Computer Methods and Programs in Biomedicine* **2022**, *224*, 106990, doi:10.1016/j.cmpb.2022.106990.
159. Li, X.; Yan, X.; Li, S.; Huang, W.; Wang, H.; Zhao, T.; Huang, M.; Zhou, N.; Shen, Y. MPicker: Visualizing and Picking Membrane Proteins for Cryo-Electron Tomography 2024.
160. Martinez-Sanchez, A.; Kochovski, Z.; Laugks, U.; Meyer Zum Alten Borgloh, J.; Chakraborty, S.; Pfeffer, S.; Baumeister, W.; Lučić, V. Template-Free Detection and Classification of Membrane-Bound Complexes in Cryo-Electron Tomograms. *Nat Methods* **2020**, *17*, 209–216, doi:10.1038/s41592-019-0675-5.
161. Himes, B.A.; Zhang, P. emClarity: Software for High-Resolution Cryo-Electron Tomography and Subtomogram Averaging. *Nat Methods* **2018**, *15*, 955–961, doi:10.1038/s41592-018-0167-z.
162. Castaño-Díez, D.; Kudryashev, M.; Arheit, M.; Stahlberg, H. Dynamo: A Flexible, User-Friendly Development Tool for Subtomogram Averaging of Cryo-EM Data in High-Performance Computing Environments. *Journal of Structural Biology* **2012**, *178*, 139–151, doi:10.1016/j.jsb.2011.12.017.
163. Navarro, P.; Scaramuzza, S.; Stahlberg, H.; Castaño-Díez, D. The Dynamo Software Package for Cryo-Electron Tomography and Subtomogram Averaging. *Microsc Microanal* **2020**, *26*, 3142–3145, doi:10.1017/S1431927620023958.
164. Balyschew, N.; Yushkevich, A.; Mikirtumov, V.; Sanchez, R.M.; Sprink, T.; Kudryashev, M. Streamlined Structure Determination by Cryo-Electron Tomography and Subtomogram Averaging Using TomoBEAR. *Nat Commun* **2023**, *14*, 6543, doi:10.1038/s41467-023-42085-w.
165. Kudryashev, M.; Castaño-Díez, D.; Deluz, C.; Hassaine, G.; Grasso, L.; Graf-Meyer, A.; Vogel, H.; Stahlberg, H. The Structure of the Mouse Serotonin 5-HT 3 Receptor in Lipid Vesicles. *Structure* **2016**, *24*, 165–170, doi:10.1016/j.str.2015.11.004.
166. Chen, W.; Kudryashev, M. Structure of RyR1 in Native Membranes. *EMBO Reports* **2020**, *21*, e49891, doi:10.15252/embr.201949891.
167. Sanchez, R.M.; Zhang, Y.; Chen, W.; Dietrich, L.; Kudryashev, M. Subnanometer-Resolution Structure Determination in Situ by Hybrid Subtomogram Averaging - Single Particle Cryo-EM. *Nat Commun* **2020**, *11*, 3709, doi:10.1038/s41467-020-17466-0.
168. Benjin, X.; Ling, L. Developments, Applications, and Prospects of Cryo-electron Microscopy. *Protein Science* **2020**, *29*, 872–882, doi:10.1002/pro.3805.